Atomic Force Microscope Measurements and Manipulation of Langmuir-Blodgett Films with Modified Tips

H. F. Knapp, W. Wiegräbe, M. Heim, R. Eschrich, and R. Guckenberger
Max Planck Institut für Biochemie, Abteilung Molekulare Strukturbiologie, D-82152 Martinsried, Germany

ABSTRACT A simple method for rendering atomic force microscope tips and cantilevers hydrophilic or hydrophobic through glow discharge in an appropriate gas atmosphere is introduced. Force curves at different humidities of these modified cantilevers were taken on freshly cleaved mica (hydrophilic surface) and on a monolayer of dipalmitoylphosphatidylethanolamine transferred onto mica (hydrophobic surface) to characterize the behavior of the cantilevers on hydrophilic and hydrophobic surfaces. Furthermore, Langmuir-Blodgett bilayers, with a dipalmitoylphosphatidylethanolamine bottom layer and a dipalmitoylphosphatidylcholine top layer, were imaged in the constant force mode in a multimode atomic force microscope in air under controlled humidity conditions. The friction and elasticity signal were recorded parallel to the topography. By varying the force exerted by the tip on the sample, different layers of the Langmuir-Blodgett system could be removed or flattened. Removal exposed underlying layers that exhibited a different friction and elasticity behavior. Furthermore, force scans with tips rendered hydrophobic were taken on the different layers of the sample to characterize the hydrophilic/hydrophobic nature of the layers. Only by combining the results obtained by the different methods can the structure of the lipid layer systems be identified.

INTRODUCTION

When scanning with the atomic force microscope (AFM) in the constant force mode, the tip is in direct contact with the sample. In this mode it is essential to minimize the force the tip is exerting on the sample in order to minimize deformations of the sample by the tip. For biological specimens, which are usually hydrophilic on their outside, a hydrophilic tip will adhere to the surface and make it difficult to control the applied force. This is especially true when scanning in air and at higher humidities. In this case a water meniscus will form between sample surface and tip (capillary condensation), pulling the tip toward the sample (Weisenhorn et al., 1989). Hydrophobic tips would greatly reduce this effect, thus enabling hydrophilic samples to be scanned at lower forces and therefore higher resolution. Commercially available AFM tips, when used directly without additional treatment, are undefined in their hydrophilic/hydrophobic nature because they can be more or less contaminated with hydrocarbons. Some groups "clean" their tips either by UV-light irradiation or by glow discharge in an air plasma. In both cases the hydrocarbons contaminating the surface of the tips are removed by cracking the contaminating long-chained hydrocarbons into smaller, volatile bits. Cleaning in an air plasma might also introduce charges on the tip surface. After these cleaning processes, the tips are hydrophilic and remain so unless the tip is contaminated again during scanning. Few groups functionalize or hydrophobize their tips by covering them with self-assembled monolayers (SAMs) (Nakagawa et al., 1993; Frisbie et al., 1994). Unfortunately these procedures for tip manipulation take a few hours. The method described here for tip hydrophobization takes only a few minutes and leaves the cantilever and the tip with a thin, robust layer of polymerized fluorocarbon similar to Teflon. Another interesting aspect of the hydrophilized and hydrophobized tips is their characteristic behavior on hydrophilic and hydrophobic samples. Specific areas of the sample can thus be characterized in this respect by locally taking force curves.

We used AFM tips rendered hydrophilic or hydrophobic to investigate phospholipid bilayers transferred onto freshly cleaved mica by the Langmuir-Blodgett technique (Blodgett and Langmuir, 1937). The assembly of phospholipids is an important factor in understanding the structure and function of biological entities such as cells and organelles. The hydrophobic and hydrophilic parts of the amphiphilic lipid molecules will interact differently and with different intensity with each other and with possible partners such as H_2O molecules and proteins, thereby determining the stability of cell membranes. Model bilayers formed by the Langmuir-Blodgett technique are submerged in an aqueous environment in which they are stable. Transferring the bilayers from their aqueous surrounding into air is nontrivial and may cause these layers to collapse. Samples thus prepared will comprise intact and collapsed areas. The former show uniform surfaces, occasionally displaying holes with the expected double-layer depth. These intact areas are discussed in detail elsewhere (Heim et al., 1995). We will concentrate on the identification of the structure of the collapsed areas by applying a multimode AFM (Wiegräbe et al., 1995) and the modified AFM tips. These areas show islands spread on the surface, with an approximate coverage of 30%. It was possible to dissect the lipid layers during scanning by increasing the load of the tip on the sample,

Received for publication 10 March 1995 and in final form 23 May 1995.
Address reprint requests to Dr. Helmut F. Knapp, Max Planck Institut für Biochemie, Abteilung Molekulare Strukturbiologie, Am Klopferspitz 18A, D-82152 Martinsried, Germany. Tel.: 49-89-8578-2653; Fax: 49-89-8578-2641; E-mail: knapp@vms.biochem.mpg.de.

0006-3495/95/08/708/08 $2.00

thereby exposing underlying layers. Only by evaluating the friction (Maivald et al., 1991; Radmacher et al., 1993) and elasticity (Meyer and Amer, 1990; Mate et al., 1987) images taken simultaneously with the topography can the images be interpreted correctly. Together with the force curves taken with hydrophobic tips on the different layers, a correct interpretation of the structure of the lipid layers can be given. Because the intention of this investigation was to identify the individual layers by the combination of the measured signals and the force curves obtained with hydrophobic tips, molecular resolution of the layers was not attempted.

MATERIALS AND METHODS

Tip modification and characterization

Commercial AFM cantilevers (Olympus Co. Ltd., Tokyo, Japan) were rendered hydrophilic through a 1-min glow discharge in air at 2×10^1 Pa and 1.5 kV_{eff} (10 kHz). The same cantilevers were rendered hydrophobic by subsequent glow discharge with the same parameters, but in a hexafluoropropene (HFP) (Hoechst AG, Frankfurt, Germany) atmosphere. We believe that the HFP polymerizes on the tip, cantilever, and chip holding the cantilever, thus forming a Teflon-like coating (Teflon is polymerized tetrafluoroethene). Polymerized HFP has a high melting point, is inert to oxidization, is electrically insulating, and will not be dissolved by standard organic solvents (Fieser and Fieser, 1965). Success of hydrophilization or hydrophobization was tested by placing a 1-μl H_2O droplet on the chip holding the cantilever. The droplet spread freely on the hydrophilic surface and formed almost a sphere on the hydrophobic surface (Figs. 1 *b* and *c*, respectively). Hydrophobization tests were also done by glow discharge of freshly cleaved mica, glass coverslips, and pieces of the wafer holding the cantilever chips in an HFP plasma under the same conditions as for the cantilevers. The 1-μl H_2O droplet was wiped away from the hydrophobic surfaces by exerting a mild pressure with a lint-free paper tissue. For all three samples, a subsequently deposited 1-μl H_2O droplet still showed the characteristic sphere formed on hydrophobic surfaces, indicating that the HFP polymerization layer was relatively stable mechanically. Even after immersing the HFP-treated glass coverslips into ethanol or acetone for 5 min, they maintained their hydrophobic behavior, as tested with the 1-μl H_2O droplets. This again indicates that these layers will not be dissolved by these organic solvents, as is also true for polymerized HFP.

The cantilevers were also viewed in a scanning electron microscope (SEM) in the secondary electron contrast mode. Fig. 2 shows a typical tip first rotary coated (at 60° incidence relative to the cantilever surface) with ~2 nm Pt/C before applying the hydrophobization procedure, as described above. The underlying conductive platinum/carbon (Pt/C) layer is necessary to prevent charging of the tip surface (and thus resolution loss) in the SEM electron beam. The tip radius of 15 nm (including the Pt/C layer and the polymerized HFP coating) is within the range of typical tip radii for oxide-sharpened Si_3N_4. The tips used in the experiments do not include the Pt/C layer and therefore should have a slightly decreased radius. In a hydrophobization series the plasma glow time was increased in steps of 0.5 min from 1 to 3 min. The cantilevers were then viewed from the side in the SEM. An additional layer could be discerned for the higher glow discharge times but was only barely seen for the lower glow discharge times. We thus assume the layer thickness of the polymerized HFP of the used cantilevers to be below the resolution limit of the SEM images taken (<10 nm).

Force curves at different humidities with the thus modified tips were done either on freshly cleaved mica (hydrophilic surface) or on a monolayer of dipalmitoylphosphatidylethanolamine (DPPE) transferred onto freshly cleaved mica by the Langmuir-Blodgett technique (hydrophobic surface). The monolayer on mica will form homogeneous, intact films and can be removed only at high scan forces (≈100 nN) (Heim et al., 1995). For every combination, a single cantilever was used to ensure a fixed force constant within that combination. For every force curve recorded, three subsequent force scans were averaged. Furthermore, three separate areas on the hydrophilic and hydrophobic samples were chosen for each humidity value. The snap-back values (see Fig. 3) of the three force curves were measured and averaged to obtain the final value plotted against the humidity. Snap-back values were measured only if the force curves taken approximately showed the same repulsion branch. All curves taken did not exhibit any irregularities (i.e., their general shape was as shown in Fig. 3). For each new humidity value an equilibration time of 20 min was allowed.

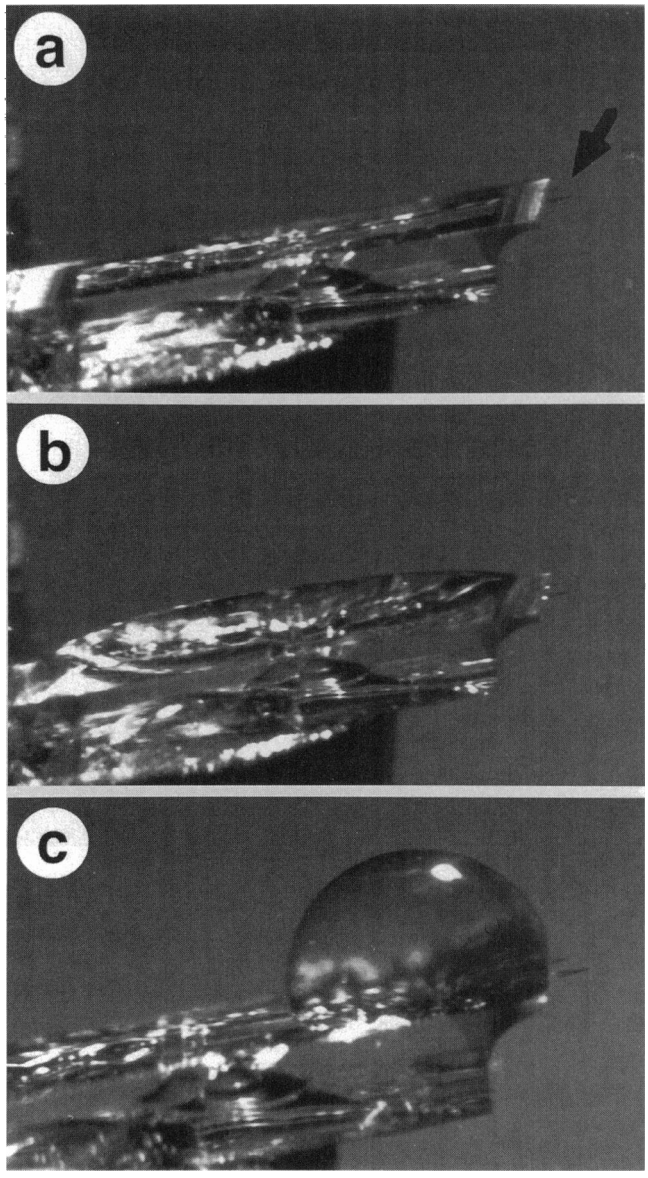

FIGURE 1 *a*) Photograph of a cantilever with chip (Olympus). The short (100 μm) and long (200 μm) cantilever available on the chip (nominal spring constant $k = 0.68$ N/m and $k = 0.16$ N/m, respectively) are indicated by the arrow. *b*) The same cantilevers rendered hydrophilic through glow discharge in an air atmosphere. A 1-μl water droplet was placed on the chip holding the cantilevers. The water droplet has freely spread across the surface (low contact angle). *c*) The same cantilevers rendered hydrophobic through glow discharge in a hexafluoropropene atmosphere. The 1-μl water droplet placed on the surface has formed almost a sphere (contact angle >90°).

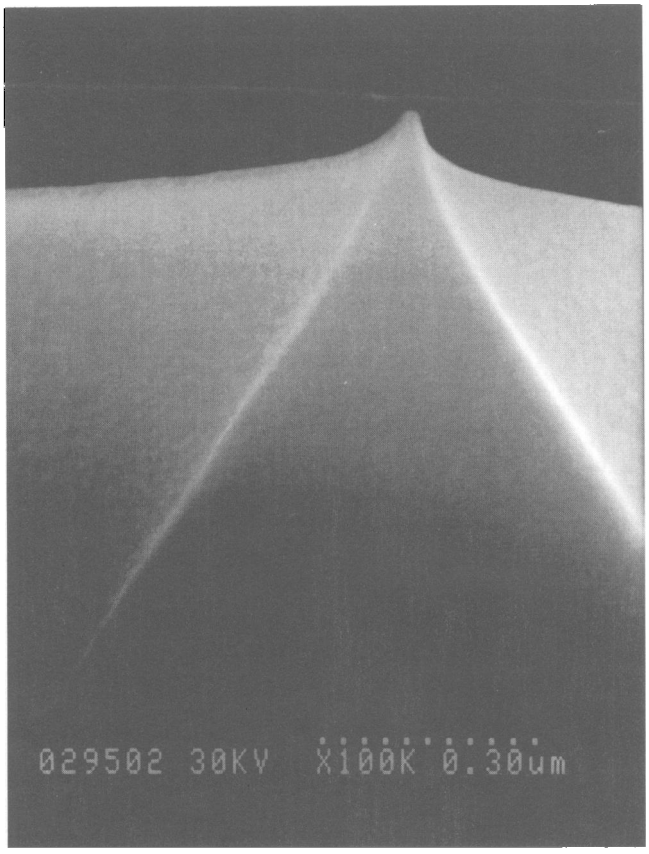

FIGURE 2 SEM image of a Si_3N_4 tip rotary coated with approximately 2 nm Pt/C at 60° incidence relative to the cantilever surface and subsequently hydrophobized for 1 min in a 2×10^1 Pa HFP plasma at 1.5 kV_{eff} (10 kHz). The conductive Pt/C layer was included to allow examination of the tip in the SEM without charging of the surface in the electron beam. The radius of the tip is 15 nm.

Lipid bilayer preparation

A sheet of freshly cleaved mica was submerged into the subphase (filtered H_2O with 18 MΩcm; Milli-Q plus system, Millipore Corporation, Bedford, MA) of a Langmuir-Blodgett trough. DPPE (Sygena, Liestal, Switzerland) dissolved in chloroform (pro analysi quality, Riedel-de Haen AG, Seelze, Germany) at 1 mg/ml was spread onto the subphase, compressed into the crystalline phase (~40 mN/m surface pressure at 20°C), relaxed for 45 min, and finally transferred onto the mica by pulling the mica sheet out of the trough at 0.1 mm/s. The subphase surface was then thoroughly cleaned before dipalmitoylphosphatidylcholine (DPPC) (Sygena) was deposited on it (1 mg/ml $CHCl_3$). The DPPC was compressed into the crystalline phase (again ~40 mN/m surface pressure at 20°C) and left to relax for another 45 min. The DPPE-coated mica was dipped back into the trough (at 0.1 mm/s), and the second layer was thereby transferred. To take the bilayer preparation from the H_2O subphase, the covered mica sheet was lifted from the trough immersed in H_2O in an appropriately sized beaker. The remaining lipid layer covering the beaker H_2O surface was removed by overflowing the beaker with added extra H_2O. The lipid-covered mica sheet was then removed from the beaker by swiftly pulling it vertically from, and oriented parallel to, the water surface. Residual water was immediately blown away with compressed air.

AFM investigation

The samples were placed into our home-built, optical beam deflection, multimode AFM (Wiegräbe et al., 1995), and the desired humidity was set in the sample compartment. The humidity became stable after 20 min, and AFM scanning was commenced. Scanning of images was done in the constant force mode, and topography, friction, and elasticity signal were recorded simultaneously in trace and retrace. Topography and friction are recorded by evaluating the individual deflections of the laser beam (due to deflection and twisting of the cantilever, respectively) on a quadrant photo diode. The long axis of the cantilever is aligned with the slow scan direction to separate topography from friction. For the elasticity signal, the sample was periodically moved (wobbled) up and down at kiloHertz frequencies and with amplitudes in the few nanometer range, and the response of the cantilever to the sample wobble was recorded by lock-in techniques. For all experiments in this report, Olympus oxide-sharpened triangular cantilevers (200-μm long, 800-nm thick) taken from one 35-chip strip as delivered by Olympus were used. All force values given were calculated using the nominal spring constant of these cantilevers (0.16 N/m).

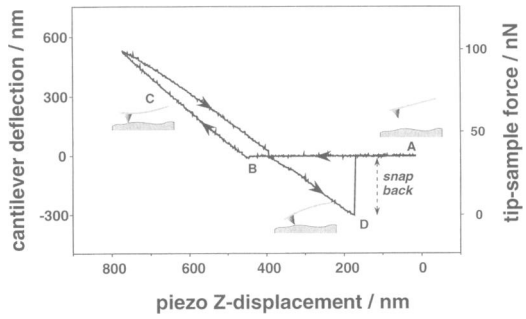

FIGURE 3 Sample force curve taken in an air atmosphere. The deflection of the cantilever is calculated into force values with the nominal spring constant of the cantilever (force = spring constant × deflection). The zero force value is set at point D. The sample Z-displacement is not the tip sample distance. The schematics at point A and C and between B and D show the cantilever configuration at these positions.

RESULTS AND DISCUSSION

Characterization of modified tips

Fig. 3 shows a typical force curve as obtained when scanning under controlled humidity conditions in air. It also shows the bending of the cantilever in selected positions of the force scan. As the sample is approached toward the tip, there is at first no interaction and the cantilever is not deflected (*A*). The attractive interaction (e.g., van der Waals) will increase with decreasing tip-sample distance until the interaction force overcomes the stiffness of the cantilever used. The tip will then jump into contact with the sample (*B*). As the piezo Z-displacement is further increased, the tip will follow the sample one to one (*C*). The force exerted by the tip onto the sample will increase proportionally to the deflection of the cantilever (proportionality factor is the spring constant k of the cantilever). In the retracting branch of the curve, the piezo Z-displacement is decreased and the force is thus lowered again. The gap between the approaching and retracting branch in the high force region of the curve (*C*) is due to the piezo hysteresis and creep after changing direction. The sample can be retracted beyond the initial jump-in point *B* if an attractive force is present (as in this example). The snap-back value is

defined as the value in nanonewtons between the loss of contact point D and the line where there is no interaction between sample and tip (A). The loss of contact point also defines the zero force point, where no contact force is exerted on the sample by the tip. The attractive force at D is mainly caused by adhesion of a water droplet to the sample and the tip. The repulsive force at D is caused by the spring property of the cantilever (see Fig. 3) trying to pull the cantilever into its resting position.

Fig. 4 shows the averaged snap-back values versus the relative humidity for the four possible combinations of hydrophilic/hydrophobic tips with hydrophilic/hydrophobic samples. For the hydrophilic tip on the hydrophilic sample (mica), the snap-back value increases with increasing humidity (Fig. 4 *a*). Values beyond a relative humidity of 55% could not be measured because the maximum piezo Z-displacement range of our instrument (1 μm) was not enough to circle through the entire force curve. The increase of the snap-back value with relative humidity can be explained with an accumulation of adsorbed water to the hydrophilic mica surface as well as to the hydrophilic tip. The water between sample and tip will not only adhere to the two surfaces but will also try to minimize its volume (high surface tension of water), thereby exerting a force on the sample surface and the tip/lever system. As the humidity increases, the cross-section of the water meniscus between sample and tip will also increase, intensifying the force pulling the tip toward the sample. A hydrophobic tip on the same hydrophilic sample (mica) will be repelled more and more as the adsorbed water layer on the hydrophilic mica grows with increasing humidity (Fig. 4 *b*). The snap-back value will decrease and is barely seen at high humidities. For a hydrophilic tip on a DPPE monolayer (hydrophobic), the snap-back value shows no real dependence on the relative humidity (Fig. 4 *c*). Water will not adsorb to the hydrophobic surface but can adsorb to the hydrophilic tip. Because the interaction between the flat, hard DPPE monolayer on mica and the AFM tip will occur only at the foremost point of the tip, water adsorbed to the tip will not greatly influence this interaction. The variation of the snap-back value is probably caused by inhomogenities of the DPPE monolayer surface (e.g., corrugations caused by dirt or holes in the monolayer), as only three force curves on three different areas of the sample are averaged for each relative humidity value. Finally, a hydrophobic tip on a DPPE monolayer (hydrophobic) will show no humidity-dependent snap-back (Fig. 4 *d*). Here water will neither adsorb to the hydrophobic sample surface nor to the hydrophobic tip.

Because the hydrophobic tip behaves more reproducibly on hydrophilic as well as on hydrophobic samples, it was used for identification of surface areas.

AFM on the DPPC/DPPE bilayers

Fig. 5 shows a time series ($t1$ through $t5$) of the constant force, friction, and wobble response signal taken with a hydrophilic tip at 3-nN imaging force and in a dry N_2 atmosphere of a DPPC on DPPE on mica sample. The constant force sequence shows islands, 5.4 nm ± 0.2 nm (n = 4) (mean value ± SD, number of measurements) in height, scattered on an otherwise smooth surface (t1). The friction image at t1 shows no contrast except for edge

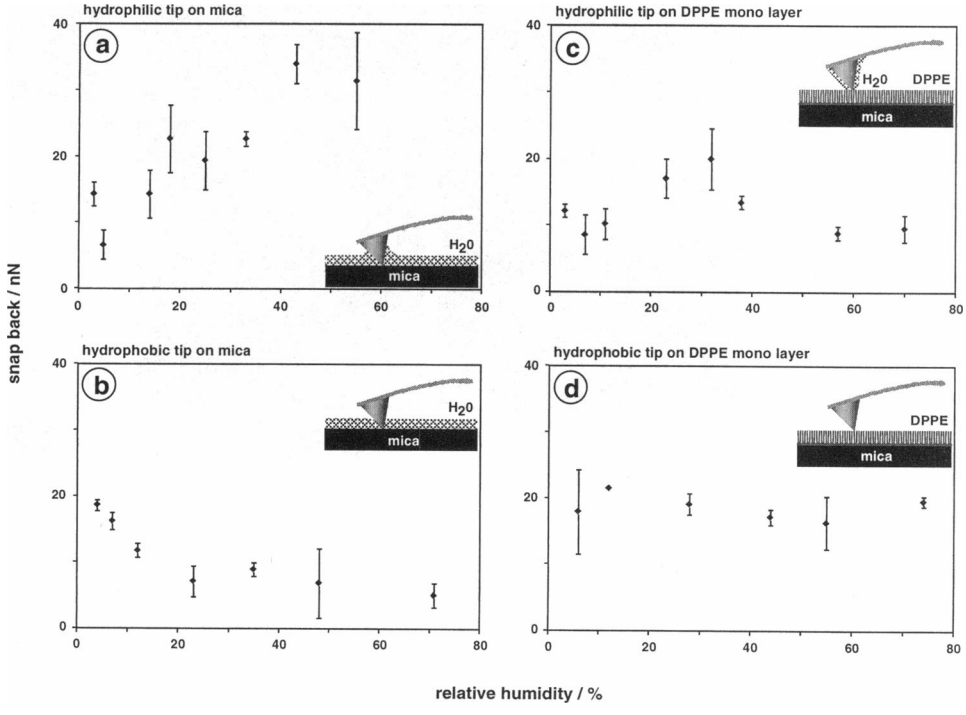

FIGURE 4 Snap-back values versus the ambient relative humidity for the four possible hydrophilic/hydrophobic tip/sample combinations. The snap back for each humidity value is averaged from the force curves at three different positions on the sample surfaces. Furthermore, for each sample position three force curves are averaged. Error bars represent the standard deviation.

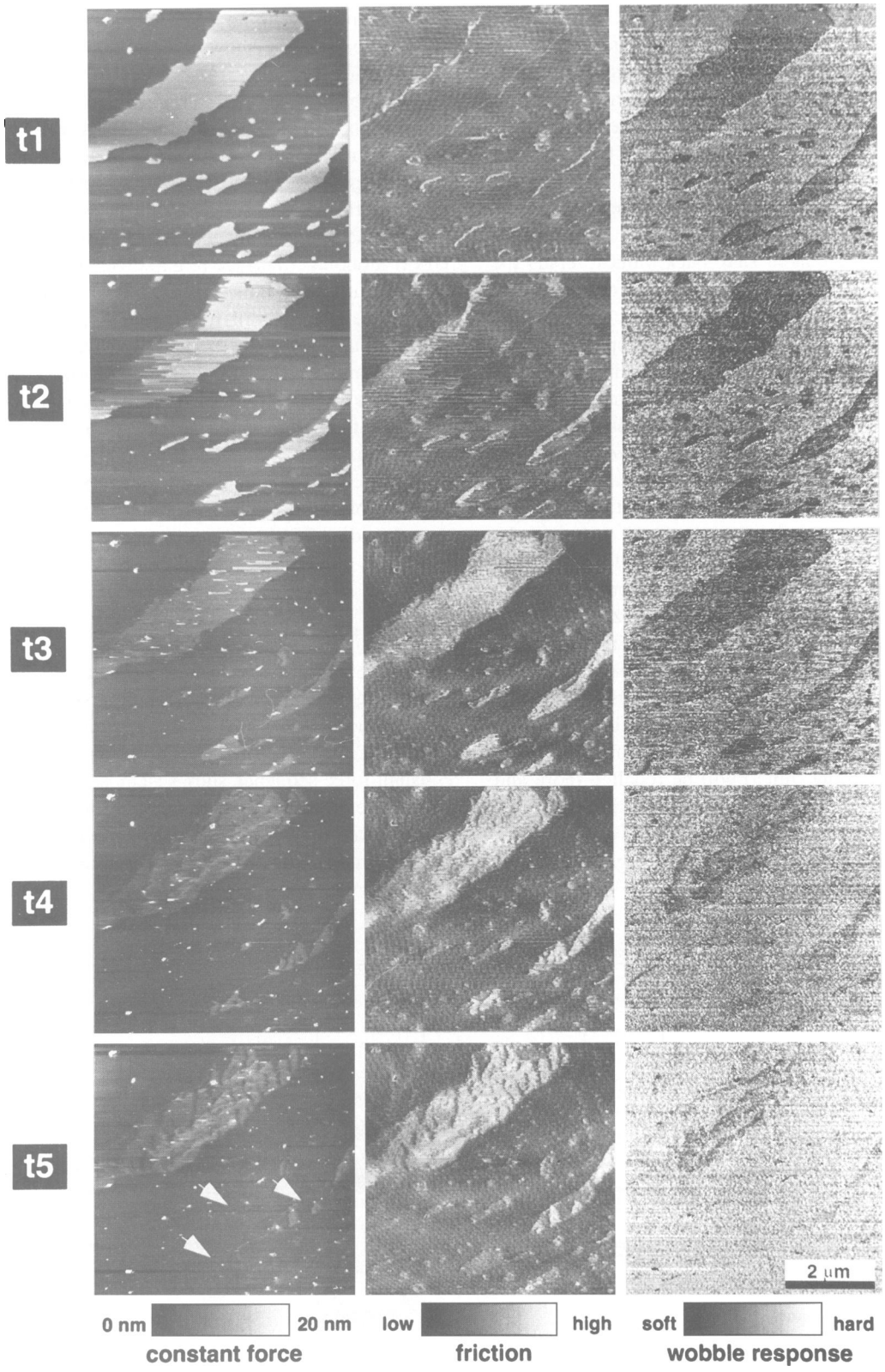

FIGURE 5 Time series (*t*1 to *t*5) showing the constant force, friction, and wobble response signal of a DPPC on DPPE on mica sample scanned with a hydrophilic tip in dry N_2 at 4 nN. Scan direction is always left to right and top to bottom. In the actual scanning process the tip scanned trace and retrace and down and up, meaning the tip scanned across the surface three times in between the frames shown here. The retrace and bottom-top images are the same, except for an island mismatch due to the hysteresis of the scanner piezo and the intrinsic inversion of the friction contrast. For the wobble response signal, the sample was periodically moved in z-direction at 10 kHz with an amplitude of 3 nm (force modulation of 0.5 nN). All data shown are raw data except for the friction images, which were Fourier filtered to remove a periodic disturbance seen as stripes diagonally progressing through the images. The apparent background increase in the wobble response series is not real but originates from an electronically induced drift in the wobble response processing unit.

effects (scan direction is left to right). The wobble response at t1 shows that the islands are softer than the surrounding surface. In frame t2 the AFM tip has partially removed a layer of the islands, revealing a second layer 2.4 nm ± 0.6 nm (n = 4) high. The friction of this second layer is definitely higher; the wobble response contrast has not changed significantly but is slightly lower. In the following scans the top layer of all islands is completely removed, and the constant force images suggest that the second layer is also removed (*arrows* in t5 point to areas of islands no longer visible). However, the high friction contrast of these islands remains. The wobble response contrast behaves analogous to the constant force contrast and gradually vanishes. Explanation of the images is as follows. Bilayer islands are scattered on a substrate, which cannot be clearly identified. The top layer of the islands is removed by scanning forces in the few nanonewton range. The bottom layer of the islands is not easily removed at these forces but is flattened by the AFM tip, like corn stalks that are flattened by a plow moving through a field of corn. This results in no topography or wobble response contrast of the bottom layer, but it will give a contrast in the friction image (viscous friction). In addition to the unidentified substrate, it is also unclear whether the head groups or the chains of the phospholipid molecules in the islands are exposed toward the AFM tip.

To identify the individual surfaces, the same sample was scanned with a hydrophobic tip at 15% relative humidity, and force curves were taken on each of the surface areas. Fig. 6 shows the constant force, friction, and wobble response images obtained after two scans over this area at 7 nN imaging force. The lower island layer is already partially exposed and flattened. Four levels in the topography image can be identified, which are labeled level 0, 1, 2, and 3 (lowest to highest). The holes (not seen in Fig. 5) are 1.8 nm ± 0.13 nm (n = 5) deep (level 1 to 0), the bottom island layer is 2.1 nm ± 0.4 nm (n = 5) high (level 1 to 2), and the total island height is 4.5 nm ± 0.3 nm (n = 4) (level 1 to 3). The higher scanning force here accounts for the reduced heights, as opposed to the one measured in Fig. 5. The friction images again show no contrast between levels 1 and 3 and a high friction on level 2 (the tip plowing through the lipids). A slightly higher friction can also be seen in the holes (level 0). The wobble response image looks different from those shown in Fig. 5. The top layer of the islands shows no contrast as compared with the surrounding level 1, whereas the bottom island layer (level 2) shows a high wobble response. The holes in level 1 also show a higher wobble response than the surrounding levels. Furthermore, the top edges of the holes and the bottom (here top and bottom are meant relative to the image frame) edges of the islands show an increased wobble response, whereas the bottom edges of the holes and the upper edges of the islands show a decreased wobble response. Fig. 7 shows representative force curves obtained on the individual levels of Fig. 6. By comparing the four force curves, one can identify the hydrophilic/hydrophobic nature of the four levels present.

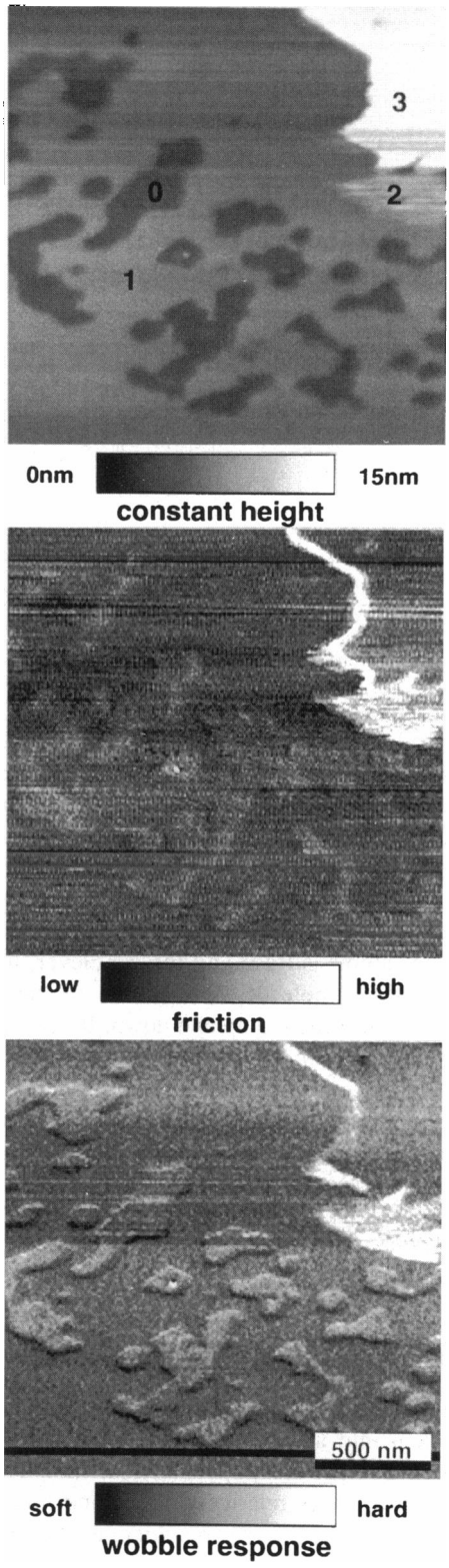

FIGURE 6 Frame 3 of a time series showing the constant force, friction, and wobble response signal of a DPPC on DPPE on mica sample scanned with a hydrophobic tip at 15% relative humidity at 7 nN. Scan direction is left to right and top to bottom. For the wobble response signal the sample was periodically moved in z-direction at 3 kHz with an amplitude of 3 nm (force modulation of 0.5 nN). The numbers in the constant force image label the four levels in this image on which the force curves of Fig. 7 were taken.

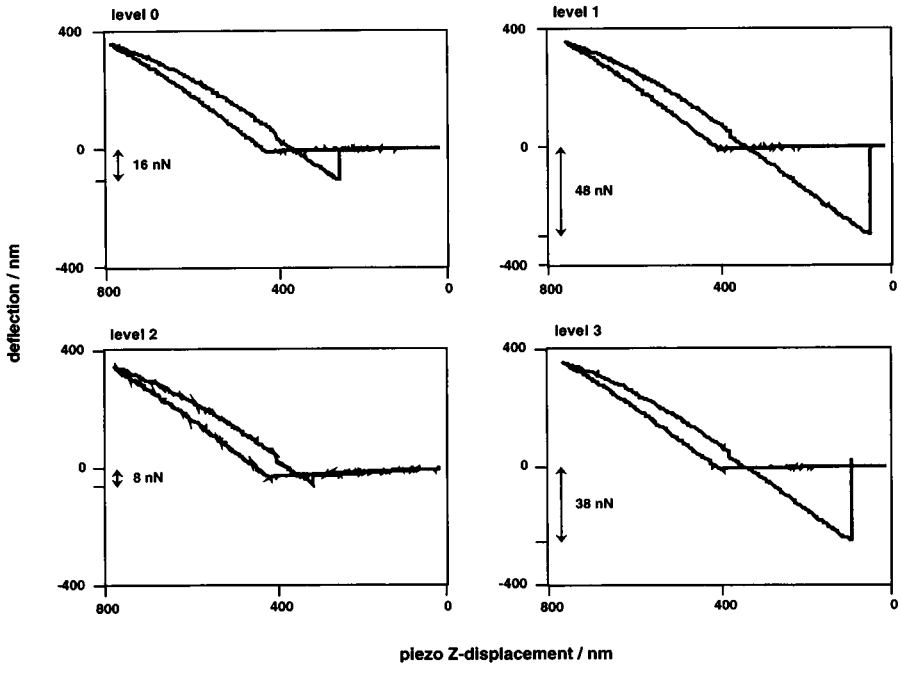

FIGURE 7 Force curves taken on the four levels labeled in Fig. 5. The dimension of the *y*-axis here is the deflection of the cantilever in nanometers to emphasize the same scaling of all four graphs. The snap-back value of each individual force curve is given in nN.

Levels 0 and 2 are hydrophilic, whereas level 2 is more hydrophilic than level 0; levels 1 and 3 are more or less equally hydrophobic. The abnormal wobble response image can be explained by the friction component, which is always present in the wobble response signal and is the dominant element in this case due to the higher scanning force (7 nN as opposed to 3 nN in Fig. 5). Because of the angle (~15°) between the sample surface and the cantilever, the tip will slide across the sample in the direction of the cantilever when the sample is moved up and down. If there is a strong interaction between tip and surface (i.e., at edges and areas of high friction), the cantilever will periodically buckle around the foremost part of the tip in the direction of the cantilever axis (Hoh and Engel, 1993), thereby contributing to the wobble response. Edges in the direction of the cantilever will show in the wobble response image (hence the top/bottom effects on holes and islands). Similarly, areas of high friction will show a high wobble response.

CONCLUSIONS

When all of the information gained by the AFM investigations is taken into account, a model of the DPPC/DPPE/mica system emerges (Fig. 8). The DPPE monolayer on top of the mica surface is relatively stable and homogeneous, although holes in this layer can sometimes be present. The monolayer can be removed only at relatively high scan forces (~100 nN). The height of this first DPPE monolayer is slightly smaller than expected from x-ray data, which was also observed by Wolthaus et al. (1994) for different saturated fatty acids and is ascribed to the reduced stiffness of the first monolayer of such systems. The force curves obtained on this first layer and in its holes also support the model of Fig. 8. The bottom of the holes seems hydrophilic, as expected of the mica surface, and the first layer seems hydrophobic, as expected of the hydrocarbon chains exposed in a DPPE monolayer supported on mica. The DPPC layer transferred onto the DPPE monolayer may collapse during the transfer from the water subphase of the Langmuir trough to air and will then fold onto itself, forming islands with bilayer height. This is supported by the close agreement with the expected monolayer and bilayer height and the force curves obtained on the two layers of these islands. The force curves identify the top island layer as hydrophobic (hydrocarbon chains of the DPPC molecules) and the lower island layer, which first has to be exposed by scratching away the top layer with the AFM, as hydrophilic (polar headgroups of the DPPC molecule). The height and friction

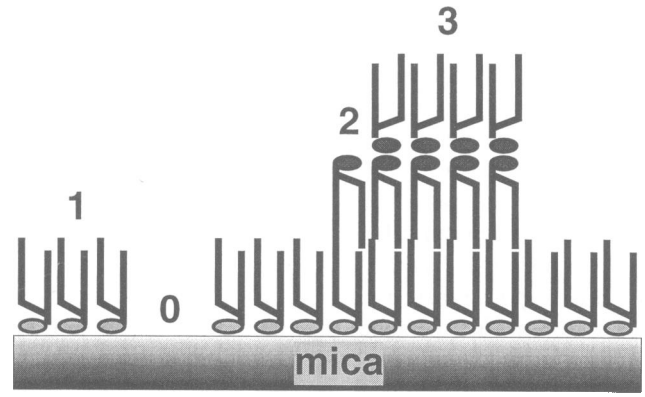

FIGURE 8 Model of the DPPC layer on DPPE layer on mica sample, prepared by Langmuir-Blodgett technique, that emerges from the studies done by AFM. The numbers correspond to the ones in Figs. 5 and 6. DPPE headgroups are shaded in light gray and DPPC head groups in dark gray. The molecule lengths are 2.5 nm for DPPE and 2.8 nm for DPPC.

images obtained on the individual levels of the system indicate that the surfaces of the layers exposing their hydrocarbon chains toward the tip are more stable than the layer exposing its headgroups because the hydrophilic surface of level 2 can be penetrated by the tip, whereas the hydrophobic surfaces stay intact (reduced height through flattening and high friction contrast through viscous friction in the former case). However, the topmost level 3 can be scratched away at low scan forces (few nanonewton range) and thus can be completely removed.

The results show that careful interpretation of the wobble response signal is necessary, as it will not always correspond to the elasticity of the investigated area. Edge effects and friction between tip and sample surface will always contribute to the wobble response. The intensity of the contribution depends on 1) the wobble amplitude and the angle between cantilever and sample surface (defines the lateral movement of the tip caused by sample wobble) and 2) the load of the tip on the sample (defines the magnitude of the friction between tip and sample).

Finally, the hydrophobized AFM tips reveal several opportunities. First of all they are quickly and easily produced through the plasma polymerization of HFP on the AFM tip and cantilever. Second, as shown here, these tips allow differentiation between hydrophilic and hydrophobic areas of the sample, thereby enabling identification of structures such as the lipid layers. Lateral resolution of this method still needs to be investigated. Interesting in this aspect is the employment of the hydrophobic tips in AFM capable of acquiring force curves at every pixel scanned (Radmacher et al., 1994; van der Werf et al., 1994). Third, the strongly reduced adhesion of hydrophobic tips on hydrophilic surface in humid atmospheres will facilitate AFM investigations in air of hydrophilic samples at low forces. Because most of the substrates used for AFM investigations of biomolecules are hydrophilic, this includes most of the systems investigated. Fully hydrated samples can thus be scanned at high humidities and low forces, but hydrophobic tips will also reduce adhesive interactions with hydrophilic samples when scanned in liquids, also increasing the resolution in this field (Franke and Keller, 1993).

Manfred Heim prepared the Langmuir-Blodgett films at the Institut für Medizinische Biophysik, Technische Universität München, Klinikum Rechts der Isar, München, Germany. We thank Robert M. Glaeser for sharing his knowledge on the hydrophobization of surfaces with us and A. Engel for fruitful discussions. We also thank Thomas Hartmann for encouraging us on the hydrophobization of AFM cantilevers. We are grateful to the Hoechst AG (Frankfurt, Germany) for supplying us with a free cylinder of hexafluoropropene.

REFERENCES

Blodgett, K. B., and I. Langmuir. 1937. Polymorphism of phospholipid monolayers. *Physiol. Rev.* 37:964.

Fieser, L., and M. Fieser. 1965. Organische Chemie. Verlag Chemie GmbH, Wienheim/Bergstrasse. 1730–1757.

Franke, F., and D. Keller. 1993. Towards high resolution imaging of DNA. *SPIE.* Vol. 1891. Advances in DNA Sequencing Technology. 78–84.

Frisbie, C. D., L. F. Rozsnyai, A. Noy, M. S. Wrighton, and C. M. Lieber. 1994. Functional group imaging by chemical force microscopy. *Science.* 265:2071–2074.

Heim, M., G. Ceve, R. Guckenberger, H. F. Knapp, and W. Wiegräbe. Lateral electrical conductivity of mica supported lipid bilayer membranes measured by STM. *Biophys J.* In press.

Hoh, J. H., and A. Engel. 1993. Friction effects on force measurements with an AFM. *Langmuir.* 9:3310–3312.

Maivald, P., H. J. Butt, S. A. C Gould, C. B. Prater, B. Drake, J. A. Gurley, V. B. Elings, and P. K. Hansma. 1991. Using force modulation to image surface elasticities with the AFM. *Nanotechnology.* 2:103.

Mate, C. M., G. M. McClelland, R. Erlandsson, and S. Chiang. 1987. *Phys. Rev. Lett.* 59:1942.

Meyer, G., and N. M. Amer. 1990. Simultaneous measurement of lateral and normal forces with an optical-beam-deflection AFM. *Appl. Phys. Lett.* 57:2089–2091.

Nakagawa, T., K. Ogawa, T. Kurumizawa, and S. Ozaki. 1993. Discriminating molecular length of chemically adsorbed molecules using an AFM having a tip covered with sensor molecules (an AFM having chemical sensing function). *Jpn. J. Appl. Phys.* 32:L294–L296.

Radmacher, M., R. W. Tilmann, and H. E. Gaub. 1993. Imaging viscoelasticity by force modulation with the AFM. *Biophys. J.* 64:735.

Radmacher, M., J. P. Cleveland, M. Fritz, H. G. Hansma, and P. K. Hansma. 1994. Mapping interaction forces with the AFM. *Biophys. J.* 66:2159–2165.

Weisenhorn, A. L., P. K. Hansma, T. R. Albrecht, and C. F. Quate. 1989. Forces in atomic force microscopy in air and water. *Appl. Phys. Lett.* 54:2651–2653.

van der Werf, K. O., C. A. J. Putman, B. G. de Grooth, and J. Greve. 1994. Adhesion force imaging in air and liquid by adhesion mode AFM. *Appl. Phys. Lett.* 65:1195–1197.

Wiegräbe, W., H. F. Knapp, H. Eberhart, R. Gatz, T. Hartmann, M. Heim, C. Lorek, and R. Guckenberger. A multifunctional SFM for biological applications. *Rev. Sci. Instrum.* In press.

Wolthaus, L., A. Schaper, and D. Möbius. 1994. Microcrystallinity of solid-state Langmuir-Blodgett films of saturated fatty acids studied by SFM and Brewster angle microscopy. *J. Phys. Chem.* 98:10809–10813.